Tunable dual-band infrared polarization filter based on a metal-dielectric-metal compound rectangular strip array

Biao Chen (陈 彪)[1], Xiahui Zeng (曾夏辉)[2], Xiyao Chen (陈曦曜)[2,*], Yuanyuan Lin (林媛媛)[1], Yishen Qiu (邱怡申)[1], and Hui Li (李 晖)[1]

[1]*College of Photonic and Electronic Engineering, Fujian Normal University, Fuzhou 350007, China*
[2]*Department of Physics and Electronic Information Engineering, Minjiang University, Fuzhou 350108, China*
**Corresponding author: chenxy2628@aliyun.com*

Received September 29, 2014; accepted December 22, 2014; posted online February 17, 2015

A tunable dual-band infrared polarization filter is proposed and investigated. Based on the perfect absorption characteristic of the metal-dielectric-metal sandwich structure, the reflection spectrum performs as a filter. The filter consists of three layers. The top layer is a compound metal nano-structure array comprised of rectangular strips. The middle and bottom layers are a dielectric spacer and metal film, respectively. The calculated results show that the filter properties are closely related to the polarization of the incident light. Different dual-band wavelengths are filtered while the incident light has different polarizations, which are parallel or vertical to the x axis. Moreover, it is found that the resonant wavelength strongly depends on the length of the rectangular strip (which causes the resonant effect) and is independent of other strips. Therefore, the filter wavelengths can be tuned freely by adjusting the length of the corresponding rectangular strip. In addition, the calculated results show that all of the intensities at the filter wavelengths are closed to zero, which implies that the filter exhibits good filtering performance.

OCIS codes: 130.0130, 130.7408, 130.3990.
doi: 10.3788/COL201513.031301.

Nanoplasmonic devices have attracted considerable interest due to their unique ability to manipulate light in sub-wavelength optics fields. In these plasmonic devices, surface plasmons (SPs)[1,2] are utilized to enhance the optical field intensity and overcome the classical diffraction limit. Recently, many devices based on SPs have been proposed and applied widely, such as plasmonic nanocavities[3], imaging systems[4,5], transistors[6,7], absorbers[8,9], and sensors[10–13]. Among these devices, absorbers have achieved rapid development (due to their ultra-strong ability of absorbing electromagnetic waves and freely tuning the absorption wavelength) since a perfect absorber was proposed[8,14–16]. Moreover, a plasmonic absorber is small. With these two properties, the absorber can be well-applied to increase the sensitivity of the detector and reduce the noise.

In order to increase the absorption efficiency, the absorbers are designed to possess wide-angle, polarization-insensitive absorption[17,18]. Much research has been done toward obtaining a better-performing absorber. During this investigative process, researchers have found that an absorber can be applied toward developing a filter which yields a reflection spectrum that performs as a filter. In 2001, a band-stop filter with a broader stop band for space transmission was realized by making use of plasmon hybridization[19].

Moreover, in 2012, a tunable plasmonic polarization filter based on a metal elliptical disc resonator was reported[20]. The frequency of the polarized light can be tuned by changing the axis ratio of the elliptical disc. Unlike the developmental trend of the absorber, the filter is designed in order to obtain polarization-dependent absorption. The resonant wavelength depends on the light polarization. However, it is obvious that the reported polarization filter only exhibits a single-band filter property. Furthermore, the elliptical shape imparts strict demands on the fabrication process and the modulation range is limited. In order to obtain a polarization filter with better performance, an asymmetrical cross-shaped structure is considered as a favorable choice because that it is sensitive to the light polarization and can be fabricated and adjusted easily[21].

In this Letter, a tunable dual-band infrared polarization filter based on a metal-dielectric-metal compound rectangular strip array is investigated by the finite difference time-domain (FDTD) method. First, a polarization filter that possesses dual-band filter properties for E_x polarization and a single band for E_y polarization is realized. Second, two asymmetrical cross resonators formed by four strips are used to realize a tunable dual-band filter for both polarizations at the same time. The calculated results show that the filtered wavelength (resonant wavelength) is strongly dependent on the length of the strip which caused the resonant effect. Thus the resonant wavelength for a different polarization can be modulated by adjusting the length of the corresponding strip. In addition, it can be seen that the filter exhibits good filtering performance in the wavelength range of interest because the intensities at the filter wavelengths are close to zero.

A schematic of the polarization filter cell structure is shown in Fig. 1. This structure can act as a polarization filter that has dual-band filter properties for E_x

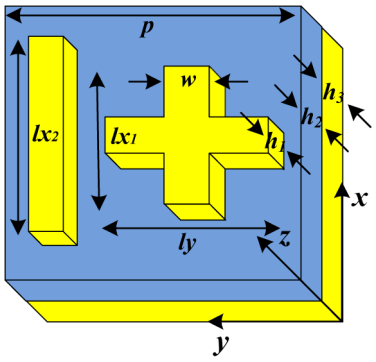

Fig. 1. Schematic of the polarization filter cell structure. Top layer is a metal compound in rectangular strips. Thickness and the width of the three rectangular strips is $h_1 = 20$ nm and $w = 100$ nm. Middle and bottom layers are MgF_2 and a gold film, respectively. Thicknesses of the MgF_2 layer and gold film are $h_2 = 50$ nm and $h_3 = 180$ nm, respectively. Dimensions of the filter cell structure in both x- and y-directions are $p = 600$ nm.

polarization and single band for E_y polarization. A tunable dual-band filter for both polarizations at the same time is discussed in a subsequent paragraph. As shown in Fig. 1, the top layer is a compound metal nano-structure array comprised of an asymmetrical cross resonator and a rectangle strip which parallels the x axis. The asymmetrical cross resonator is formed by two perpendicular rectangle strips which are parallel and vertical to the x axis, respectively. The middle and bottom layers are a dielectric spacer and metal film, respectively. The dielectric function of the metal (gold) is given by the Drude model[22]

$$\varepsilon_m(\omega) = \varepsilon_0\{1 - \omega_p^2/\omega(\omega + i\gamma)\}, \quad (1)$$

where ε_0 is the permittivity of the vacuum, the plasma wavelength $\omega_p = 1.37 \times 10^{16}$ s^{-1}, ω is the angle wavelength of the incident wave, and the damping rate $\gamma = 4.08 \times 10^{13}$ s^{-1}. In order to investigate the characteristics of the filter, the reflection spectra are simulated with the 3D FDTD method based on *EastFDTD* software[23]. In the calculations, the spatial mesh cell is set to $\Delta x = \Delta y = \Delta z = \Delta s = 5$ nm and the time step is taken as $\Delta t = \Delta s/2c = 8.3333 \times 10^{-18}$ s. The incident wave with polarization propagates along the negative z axis. Periodic boundary conditions are set in the x- and y-directions, and an open boundary is defined in the z-direction for the electromagnetic wave incidence and transmission.

Assume that the absorption, reflection, and transmission spectra are $A(\omega)$, $R(\omega)$, and $T(\omega)$, respectively. The absorption $A(\omega)$ can be obtained by $A(\omega) = 1 - R(\omega) - T(\omega)$. The transmission $T(\omega)$ is zero in the entire investigated wavelength range because that ground plane is metal, thus the absorptivity $A(\omega) = 1 - R(\omega)$. When $R(\omega)$ is zero, the structure becomes a perfect absorber. And it is known that the zero $R(\omega)$ is caused by the destructive interference between the direct reflection of an asymmetrical cross resonator array and the subsequent multiple reflections of the dielectric spacer and metal layer[24], and the light is trapped in the dielectric layer[25].

Figure 2 presents the reflection spectra with different light polarizations of a polarization filter as shown in Fig. 1. It is easily found that the reflection spectrum of the E_x polarization has two dips in the wavelength range of interest and the wavelengths of the two dips are 1310 and 2000 nm, respectively. On the other hand, the reflection spectrum of the E_y polarization has one dip which is located at 1516 nm. The reflectivities of the reflection dips are close to zero (0.012 of 1310 nm and 0.052 of 2000 nm for E_x polarization, and 0.003 of 1516 nm for E_y polarization). On the other hand, it is found that the reflectivity of the reflection spectrum corresponding to E_x (E_y) at the resonant dip wavelength of the other polarization E_y (E_x) is over 0.8. This indicates that the filter has strong polarization selectivity.

For well-recognized the characters of the resonant dips, the distributions of the electric field of $\mathbf{E_z}$ at the surface of metal compound rectangle strips at the wavelengths of the three dips, 1310 and 2000 nm for E_x polarization and 1516 nm for E_y polarization, are depicted in Fig. 3. From Figs. 3(a) and 3(b), we can see that the electric fields at 1310 and 2000 nm for E_x polarization are almost distributed at the edges of the gold rectangle strip l_{x1} and l_{x2}, respectively. There is negligible distribution of the electric field at the vertical gold strip.

That is to say, the gold strip of the asymmetrical cross resonator vertical to the light polarization has no effect on the resonant wavelength of E_x. From Fig. 3(c), we can observe the similar character at 1516 nm for E_y polarization. The previous discussions reveal a fact that the wavelength of the reflection dip of the filter can be modulated only by changing the parameters of the corresponding gold strip.

On the other hand, it is known that the metal surface charges (SPs) can be deduced from the electric field distribution[26]. So the electric field distribution can present the distribution of the charge oscillation. That is to say, Fig. 3 equivalently indicates the charge oscillation. According to the electric dipole resonance frequency formula[27]

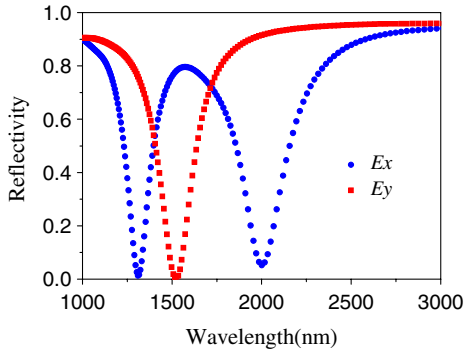

Fig. 2. Simulated reflection spectra of the filter with $l_{x1} = 300$ nm, $l_{x2} = 450$ nm, and $l_y = 350$ nm for E_x and E_y polarization.

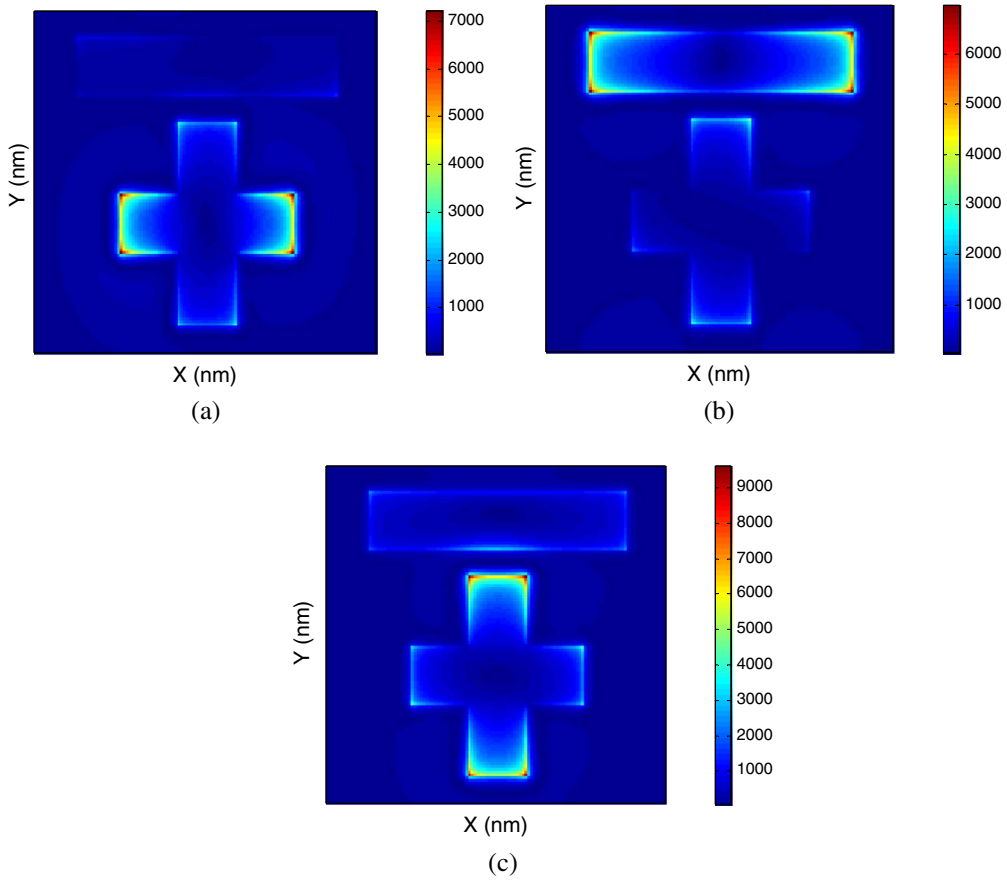

Fig. 3. Distributions of the electric field $\mathbf{E_z}$ at the surface of the metal compound rectangular strips corresponding to the following; E_x polarization at the resonant dip (a) 1310 and (b) 2000 nm; (c) E_y polarization at the resonant dip 1516 nm.

$$\omega_e \propto c/2L\sqrt{\varepsilon_{\text{eff}}}, \tag{2}$$

where c is the vacuum speed of light, L is the charge oscillating length, and ε_{eff} is the equivalent permittivity near the metal rectangle strips (where charge exists, the resonant wavelength is proportional to the oscillating length). As shown in Fig. 2, the ratio of l_{x1}, l_{x2}, and l_y is 1.00:1.50:1.16. The ratio of the corresponding resonant wavelength is 1.00:1.52:1.16. It is in accordance with the theory formula. Because the electric field is only distributed at the edges of the gold rectangle strip which caused the resonant effect, and the resonant wavelength is proportional to the length of the corresponding rectangle strip, it opens an accurate and simple way to tune the filtered wavelength freely.

Figure 4(a) presents the reflection spectra of the filter for E_x polarization of the rectangle strips with different length l_{x1}. The values of l_{x2} and l_y are fixed at 450 and 350 nm, respectively. It is found that when l_{x1} increases from 280 to 320 nm with every step of 20 nm, the shorter

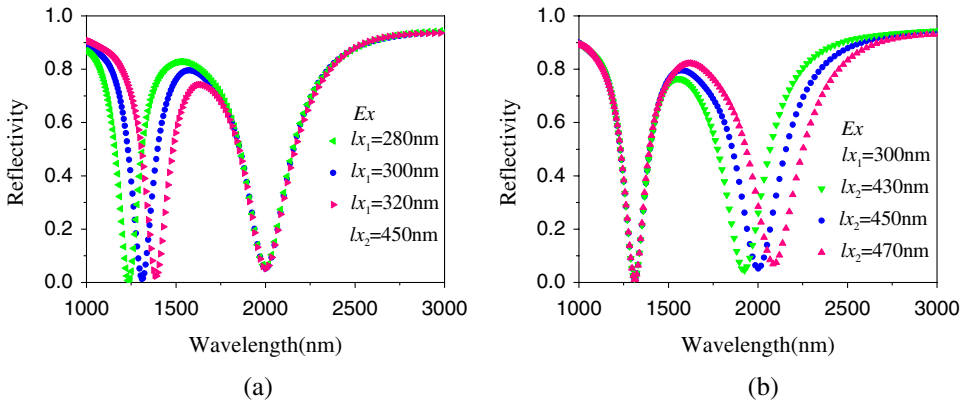

Fig. 4. Simulated reflection spectra of the filter structure as a function of the length; (a) l_{x1} with $\Delta l_{x1} = 20$ nm and l_{x2} is fixed at 450 nm; (b) l_{x2} with $\Delta l_{x2} = 20$ nm and l_{x1} is fixed at 300 nm for E_x polarization.

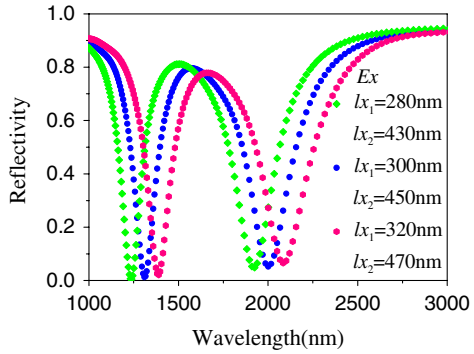

Fig. 5. Simulated reflection spectra of the filter structure as a function of the length of the gold strips l_{x1} and l_{x2} with every step of 20 nm at the same time, and l_y is fixed at 350 nm for E_x polarization.

resonant wavelength for E_x polarization exhibits a redshift; however, the longer resonant wavelength 2000 nm for E_x polarization does not change. By fixing $l_{x1} = 300$ nm and $l_y = 350$ nm, and changing l_{x2} from 430 to 470 nm with every step of 20 nm, we can get similar results, as shown in Fig. 4(b).

Moreover, we can change the lengths of l_{x1} and l_{x2} at the same time. When l_{x1} and l_{x2} change from 280 and 430 nm, respectively, to $l_{x1} = 320$ nm and $l_{x2} = 470$ nm, respectively, with every step of 20 nm, while l_y is fixed at 350 nm, the reflection spectra of the filter for E_x polarization can be determined (Fig. 5). It is shown that the two resonant wavelengths exhibit a redshift at the same time. The resonant wavelengths are the same with that shown in Fig. 4 while the corresponding rectangular strip has the same length. Meanwhile, the reflection spectra for E_y polarization are shown in Fig. 6. It can be seen that the wavelength of the resonant dip does not change. From Figs. 5 and 6, we can see that the filter wavelength is strongly dependent on the length of the rectangular strips which is in accordance with the light polarization and is independent of the length of the vertical one.

From the previous discussions, we have shown a tunable polarization filter that exhibits a dual-band filter property

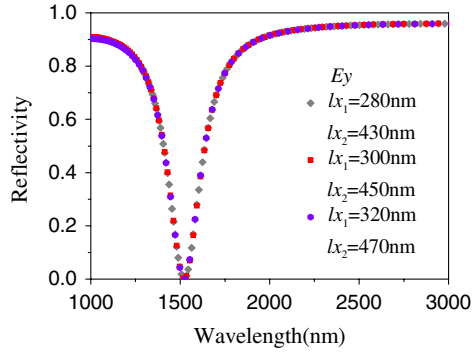

Fig. 6. Simulated reflection spectra of the filter structure as a function of the length of the gold strips l_{x1} and l_{x2} with every step of 20 nm at the same time, and l_y is fixed at 350 nm for E_y polarization.

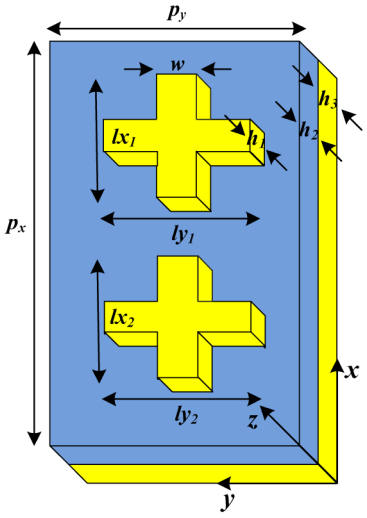

Fig. 7. Schematic of the dual-band polarization filter cell structure. Top layer is two gold asymmetrical cross resonators. Thickness and the width of the four rectangle strips is $h_1 = 20$ nm and $w = 100$ nm. Middle and bottom layers are MgF_2 and gold films, respectively. Thicknesses of the MgF_2 layer and gold film are $h_2 = 70$ nm and $h_3 = 180$ nm, respectively. Dimensions of the filter cell structure are $p_x = 1000$ nm and $p_y = 600$ nm along the x- and y-directions, respectively.

for E_x polarization and a single band for E_y polarization. Then, a tunable dual-band filter for both polarizations at the same time is realized by using two asymmetrical cross resonators. A schematic cell structure of the dual-band filter is shown in Fig. 7.

Figure 8 shows the reflection spectra with different light polarizations of the dual-band filter. Moreover, we can change the four resonant wavelengths for both polarizations freely by adjusting the corresponding length of the branch of the asymmetrical resonator at the same time. As shown in Fig. 9, when l_{x1} and l_{x2} change from 280 and 420 nm, to $l_{x1} = 320$ nm and $l_{x2} = 460$ nm, with every step of 20 nm, and l_{y1} and l_{y2} are fixed, the two filtered wavelengths corresponding to E_x polarization exhibit a redshift. When l_{y1} and l_{y2} change from 340 and 490 nm, to $l_{y1} = 380$ nm and $l_{y2} = 530$ nm, with every step of 20 nm, and l_{x1} and l_{x2} are fixed, the two filtered

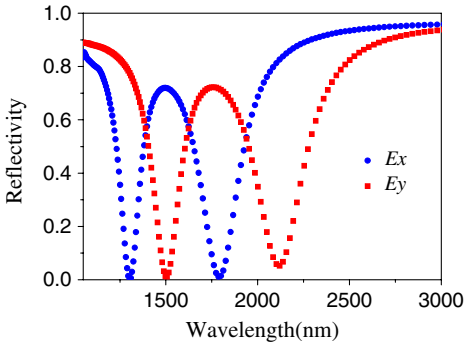

Fig. 8. Simulated reflection spectra of the filter with $l_{x1} = 300$ nm, $l_{x2} = 440$ nm, $l_{y1} = 360$ nm, and $l_{y2} = 510$ nm for E_x and E_y polarization.

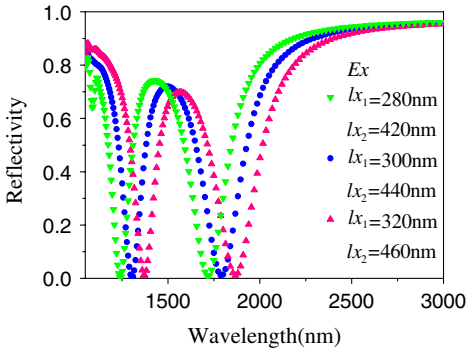

Fig. 9. Simulated reflection spectra of the filter structure as a function of the length of the gold strips l_{x1} and l_{x2} with every step of 20 nm at the same time, while l_{y1} and l_{y2} are fixed at 340 and 490 nm, respectively, for E_x polarization.

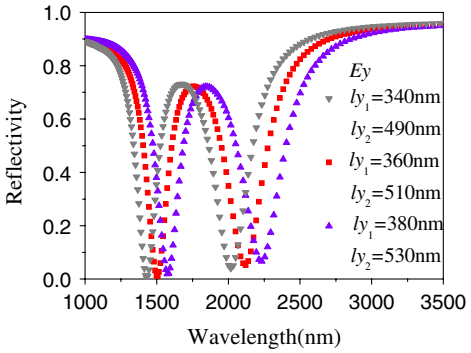

Fig. 10. Simulated reflection spectra of the filter structure as a function of the length of the gold strips l_{y1} and l_{y2} with every step of 20 nm at the same time, while l_{x1} and l_{x2} are fixed at 300 and 440 nm, respectively, for E_y polarization.

wavelengths corresponding to E_y polarization exhibit a redshift, as shown in Fig. 10.

In conclusion, a tunable dual-band infrared polarization filter based on a metal-dielectric-metal compound rectangular strip array is proposed and investigated. First, a polarization filter that possesses dual-band filtering properties for E_x polarization and a single band for E_y polarization is realized. Based on the analysis of the distributions of the electric field $\mathbf{E_z}$ at the surface of the metal compound rectangular strips at the filtered wavelength (resonant wavelength), it is found that the resonant wavelength only depends on the length of the rectangular strip which caused the resonant effect. Therefore, the filter wavelength can be tuned freely for different light polarizations by adjusting the length of the corresponding rectangular strip. Second, two asymmetrical cross resonators are used to yield a tunable dual-band filter for both polarizations at the same time. And the calculated results show that the filtered wavelength can be tuned freely. In addition, the calculated results show that all the intensities at the filter wavelengths are closed to zero, which implies that the filter exhibits good filtering performance.

This work was supported in part by the Natural Science Foundation of China (Nos. 61178089 and 51277091) and the Natural Science Foundation of Fujian Province of China (No. 2013J05095).

References

1. W. L. Barnes, A. Dereux, and T. W. Ebbesen, Nature **424**, 824 (2003).
2. E. Ozbay, Science **311**, 189 (2006).
3. G. H. Li, X. S. Chen, B. Ni, O. P. Li, L. J. Huang, Y. Jiang, W. D. Hu, and W. Lu, Nanotechnol. **24**, 205702 (2013).
4. R. Esteban, R. Vogelgesang, J. Dorfmüller, A. Dmitriev, C. Rockstuhl, C. Etrich, and K. Kern, Nano Lett. **8**, 3155 (2008).
5. G. J. Nusz, S. M. Marinakos, S. Rangarajan, and A. Chilkoti, Appl. Opt. **50**, 4198 (2011).
6. N. Guo, W. D. Hu, X. S. Chen, L. Wang, and W. Lu, Opt. Express **21**, 1606 (2013).
7. L. Wang, W. D. Hu, J. Wang, X. D. Wang, S. W. Wang, X. S. Chen, and W. Lu, Appl. Phys. Lett. **100**, 123501 (2012).
8. N. I. Landy, S. Sajuyigbe, J. J. Mock, D. R. Smith, and W. J. Padilla, Phys. Rev. Lett. **100**, 207402 (2008).
9. J. Hendrickson, J. P. Guo, B. Y. Zhang, W. Buchwald, and R. Soref, Opt. Lett. **37**, 371 (2012).
10. N. Liu, M. Mesch, T. Weiss, M. Hentschel, and H. Giessen, Nano Lett. **10**, 2342 (2010).
11. G. H. Li, X. S. Chen, O. P. Li, C. X. Shao, Y. Jiang, L. J. Huang, B. Ni, W. D. Hu, and W. Lu, J. Phys. D **45**, 205102 (2012).
12. Y. Wu and Z. Gu, Chin. Opt. Lett. **10**, 081301 (2012).
13. H. Xu, H. Li, and G. Xiao, Chin. Opt. Lett. **11**, 042401 (2013).
14. G. Q. Liu, Z. Q. Liu, Y. H. Chen, Z. J. Cai, Y. Hu, X. N. Zhang, and K. Huang, Sci. Adv. Mater. **6**, 1099 (2014).
15. Z. Q. Liu, H. B. Shao, G. Q. Liu, X. S. Liu, H. Q. Zhou, Y. Hu, X. N. Zhang, Z. J. Cai, and G. Gu, Appl. Phys. Lett. **104**, 081116 (2014).
16. Z. Q. Liu, G. Q. Liu, X. S. Liu, G. L. Fu, and M. L. Liu, IEEE Photon. Technol. Lett. **26**, 2111 (2014).
17. L. Li, Y. Yang, and C. H. Liang, J. Appl. Phys. **110**, 063702 (2011).
18. P. V. Tuong, J. W. Park, J. Y. Rhee, K. W. Kim, W. H. Jang, H. Cheong, and Y. P. Lee, Appl. Phys. Lett. **102**, 081122 (2013).
19. X. Li, L. Y. Yang, C. G. Hu, X. G. Luo, and M. H. Hong, Opt. Express **19**, 5283 (2011).
20. M. N. Abbas, C. C. Wen, C. Y. Chung, and M. H. Shih, Nanotechnology **23**, 444007 (2012).
21. J. J. Cadusch, T. D. James, and A. Roberts, Opt. Express **21**, 28450 (2013).
22. M. A. Ordal, L. L. Long, R. J. Bell, S. E. Bell, R. R. Bell, R. W. Alexander, Jr., and C. A. Ward, Appl. Opt. **22**, 1099 (1983).
23. *EastFDTD v2.0* (Dongjun Science and Technology, China).
24. H. T. Chen, Opt. Express **20**, 7165 (2012).
25. X. L. Liu, T. Starr, A. F. Starr, and W. J. Padilla, Phys. Rev. Lett. **104**, 207403 (2010).
26. M. D. He, J. Q. Liu, Z. Q. Gong, Y. F. Luo, and X. S. Chen, Solid State Commun. **150**, 104 (2010).
27. W. J. Padilla, A. J. Taylor, C. Highstrete, M. Lee, and R. D. Averitt, Phys. Rev. Lett. **96**, 10740 (2006).